Liquid Crystals
Publication details, including instructions for authors and subscription information:
http://www.informaworld.com/smpp/title~content=t713926090

Side-chain cholesteric liquid crystalline elastomers containing isosorbide as chiral agent - synthesis and characterisation

Xiao-Zhi He[a]; Bao-Yan Zhang[a]; Wen-Wen Ma[a]; Lin Zhang[a]
[a] Center for Molecular Science and Engineering Northeastern University, Shenyang, People's Republic of China

To cite this Article He, Xiao-Zhi , Zhang, Bao-Yan , Ma, Wen-Wen and Zhang, Lin(2009) 'Side-chain cholesteric liquid crystalline elastomers containing isosorbide as chiral agent - synthesis and characterisation', Liquid Crystals, 36: 8, 847 — 854
To link to this Article: DOI: 10.1080/02678290903078842
URL: http://dx.doi.org/10.1080/02678290903078842

Liquid Crystals,
Vol. 36, No. 8, August 2009, 847–854

Taylor & Francis
Taylor & Francis Group

Side-chain cholesteric liquid crystalline elastomers containing isosorbide as chiral agent – synthesis and characterisation

Xiao-Zhi He, Bao-Yan Zhang*, Wen-Wen Ma, Lin Zhang and Qiang-Mu

Center for Molecular Science and Engineering Northeastern University, Shenyang 110004, People's Republic of China

(Received 18 September 2008; final form 29 May 2009)

In this work the new-style nematic monomer $\mathbf{M_1}$, chiral crosslinking reagent $\mathbf{M_C}$ and a series of new side-chain cholesteric liquid crystalline elastomers derived from $\mathbf{M_1}$ and $\mathbf{M_C}$ were prepared. The effect of the content of the chiral crosslinking unit on phase behaviour of the elastomers has been discussed. Polymer $\mathbf{P_1}$ showed nematic phase, $\mathbf{P_2}$–$\mathbf{P_7}$ showed cholesteric phase, $\mathbf{P_3}$ formed Grandjean texture in the heating cycle and turned out a blue Grandjean texture in the cooling cycle, $\mathbf{P_2}$–$\mathbf{P_3}$ with less than 6 mol% of chiral crosslinking agent gave rise to selective reflection. The elastomers containing less than 15 mol% of the crosslinking units displayed elasticity, reversible phase transition and high thermal stability. Experimental results demonstrated that the glass transition temperatures reduced first and then increased, and the isotropisation temperatures and the mesophase temperature ranges decreased with increasing content of crosslinking unit.

Keywords: Grandjean blue texture; chiral; crosslinking reagent; elastomers

1. Introduction

Liquid crystalline elastomers (LCEs) have been known for several years. The first example of a neat side-chain liquid crystalline elastomer appeared in the literature in 1981 and semi-flexible main-chain-based LC networks were also reported later, in 1986, by Zentel and Reckert. LCEs are one of the supramolecular systems, which combine the properties of LC phase with rubber elasticity (*1–7*). Their most outstanding characteristic of mechanical orientability can be applied in many fields. Also, photosetting or thermosetting of cholesteric polymers may be of interest as colourful lacquers, pigments or films, when they are capable of forming a Grandjean texture with a selective reflection of visible light. Furthermore the Grandjean (GJ) texture and its optical properties should be fixed. The fixation of the GJ texture can in principle be achieved by three different methods: a) by freezing the GJ texture below the glass transition temperatures; b) by photocrosslinking, when suitable reactive groups are present and when the GJ texture survives the photocure; c) by thermally or chemically induced crosslinking. In this study, isosorbide as chiral and crosslinking agent was introduced and the GJ textures were expected (*8–17*).

Our teams have done much research work in the field of cholesteric LCEs (*18–20*). In our previous study, short chiral crosslinking was contributed into LCE and GJ textures were obtained (*21*). Now a new side-chain cholesteric LCE derived from nematic liquid crystalline monomer: 4-Allyloxy-benzoic acid-4-[3-[4-hepty oxy-phenyl]-propionyloxy]-phenylester (M1), and long chiral crosslinking agent: hexahydrofuro[3,2-b]furan-3,6-diyl-bis[4-[3-[4-Allyloxy]phenyl] propanoyloxy]benzoate (MC) have been synthesized. The reason we chose isosorbide is that it possesses a high twisting power and obviously a high molar fraction of isosorbide generated helixes with a pitch which is too small (or large) for an interaction with visible light [22]. However, to the best of our knowledge, few cholesteric LCE materials bearing chiral crosslinking agents have been described so far. It is necessary to synthesis various chiral crosslinking and discuss the properties of chiral LCEs and look for a useful conclusion. The chemical structure of the monomers and polymers obtained were confirmed by FTIR and 1H NMR spectroscopy. The mesomorphic properties of them were investigated by differential scanning calorimetry (DSC), thermogravimetric analyse (TGA), polarizing optical microscopy (POM), and X-ray diffraction (XRD) measurement.

2. Methods

2.1 Materials

Hydroquinol was purchased from Beijing Chemical Industry Co.(China). 3-Bromopropene and Bromoheptane was purchased from Beijing Fuxing Chemical Industry Co.(China). Isosorbide was bought from Yangzhou Shenzhou new material Co. Ltd (China). 4-hydroxyl benzoic acid was purchased

*Corresponding author. Email: baoyanzhang@hotmail.com

ISSN 0267-8292 print/ISSN 1366-5855 online

DOI: 10.1080/02678290903078842
http://www.informaworld.com

from Shenyang Xinxi Chemical Reagent Company (China). 3-(4-hydroxyphenyl)propanoic acid was obtained from Shanghai Jia Chen Chemical Reagent Company. Polymethylhydrosiloxane (PMHS, Mn = 700–800) was purchased from Jilin Chemical Industry Co.(China). Toluene used in the hydrosilication reaction was first refluxed over sodium and then distilled under nitrogen. All other solvents and regents were purified by standard methods.

2.2 Characterisation

IR spectra were measured on a Perkin Elmer Spectrum One FT-IR spectrometer (Perkin Elmer Instruments, USA). ^{1}H NMR spectra (300 MHZ) were recorded on a Varian WH-90PFT spectrometer. Phase transition temperatures and thermodynamic parameters were determined by Netzsch DSC 204 (Netzsch, Germany) with a liquid nitrogen cooling system. The thermal stability of the polymers was measured with a Netzsch TGA 209C thermogravimetric analyzer. The heating and cooling rates were 10°C min^{-1}. A Leica DMRX (Leica, Germany) polarising optical microscope equipped with a Linkam THMSE-600 (Linkam, England) hot stage was used to observe phase transition temperatures and analyze LC properties for the monomers and polymers through observation of optical textures. XRD measurements were performed with a nickel-filtered Cu-K_α (λ = 0.1542 nm) radiation with a DMAX-3A Rigaku (Rigaku, Japan) powder diffractometer.

2.3 Synthesis of the monomers

The synthesis of the olefinic monomers is shown in Scheme 1.

2.3.1 Synthesis of 4-allyloxy-benzoic acid-4-[3-[4-heptyloxy-phenyl]propionyloxy]phenylester (M_1)

2.3.1.1 Synthesis of 3-[4-heptyloxy-phenyl]propionic acid Potassium hydroxide (0.1 mol) and potassium iodide (0.003 mol) were dissolved in 150 ml water to obtain an aqueous solution, which was then added to a mixture of 3-(4-hydroxyphenyl)propanoic acid (0.1 mol) and ethanol (200 ml). *n*-Bromoheptane (0.12 mol) was then added dropwise and the mixtures were stirred at room temperature for 2 h. They were then refluxed for 24 h. The cold reaction mixture was precipitated into hydrochloric acid aqueous solution, and the precipitated product was washed with water and isolated by filtration, recrystallised from ethanol, and then dried overnight under vacuum to obtain a yellow powder (21.1 g, yield = 80%, mp = 60°C).

2.3.1.2 Synthesis of 4-allyloxy-benzoic acid 4-hydroxy-phenylester Hydroquinol (0.25 mol) was dissolved in a mixture of anhydrous pyridine (10 ml) and tetrahydrofuran (100 ml). 4-Allyloxy benzoic acid chloride (0.05 mol) (lab synthesised) was then added at once and the reaction mixture was refluxed for 24 h. The cold reaction mixture was precipitated into hydrochloric acid aqueous solution, and the precipitated product was washed with hot water and isolated by filtration, and was then recrystallised from ethanol. White solid powders were obtained (14.2 g, yield = 56%, mp = 144°C).

2.2.1.3 Synthesis of 4-allyloxy-benzoic acid-4-[3-[4-heptyloxy-phenyl]-propionyloxy]phenylester (M_1) 4-Allyloxybenzoic acid 4-hydroxy phenyl ester (0.1 mol) was dissolved in a mixture of dry pyridine (10 ml) and dry tetrahydrofuran (100 ml). 3-(4-Hydroxyphenyl)propanoic acid chloride (0.1 mol) (lab synthesised) was then added at once and the reaction mixtures were refluxed for 32 h. The cold reaction mixtures were precipitated into hydrochloric acid aqueous solution, and the precipitated product was washed with water and isolated by filtration, and was then recrystallised from intermixture of acetone and ethanol. Yellow solid powders were obtained (42.5 g, yield = 85%, mp = 62°C).

IR (KBr): 3097, 3039 (=C–H), 2980–2850 (CH_3, CH_2),1735 (C=O), 1649 (C=C), 1605–1450 cm^{-1} (Ar-).

^{1}H NMR ($CDCl_3$): δ 0.88–0.92 (t, 3H, -CH_3), 1.27–1.80 (m, 10H, -CH_2-), 2.84–3.04 (t,4H,-CH_2-CH_2-), 3.92–3.94 (t, 2H, -CH_2-O-), 4.63–4.64 (d, 2H, -CH_2O-), 5.33–5.47(m, 2H, CH_2=CH-), 6.04–6.11 (m, 1H, CH_2=CH-), 6.85–8.15 (m, 12H, Ar-H).

2.3.2 Synthesis of hexahydrofuro[3,2-b]furan-3,6-diyl-bis[4-[3-[4-ally-loxy phenyl] propanoyloxy] benzoate (M_C)

A few drops of N, N-dimethylformamide (DMF) was added to a suspension of 4-[3-[4-allyloxy-phenyl]propionyloxy]benzoic acid (0.1 mol) in freshly distilled thionyl chloride (40 ml) and the reaction mixtures were refluxed for 5 h and then the excess thionyl chloride was removed under reduced pressure to give the corresponding acid chloride. Isosorbide was dissolved in a mixture of dry triethylamine (10 ml) and chloroform (100 ml); the 4-[3-[4-allyloxy-phenyl]propionyloxy]benzoic acid chloride was then added at once in an ice bath, and then the reaction mixture was refluxed for 72 h. The cold reaction mixtures were precipitated into water, the precipitated product was isolated by filtration and recrystallised from ethanol (yield = 85%, mp = 90°C, $[\alpha]_{589}^{20}$ = –16.9°).

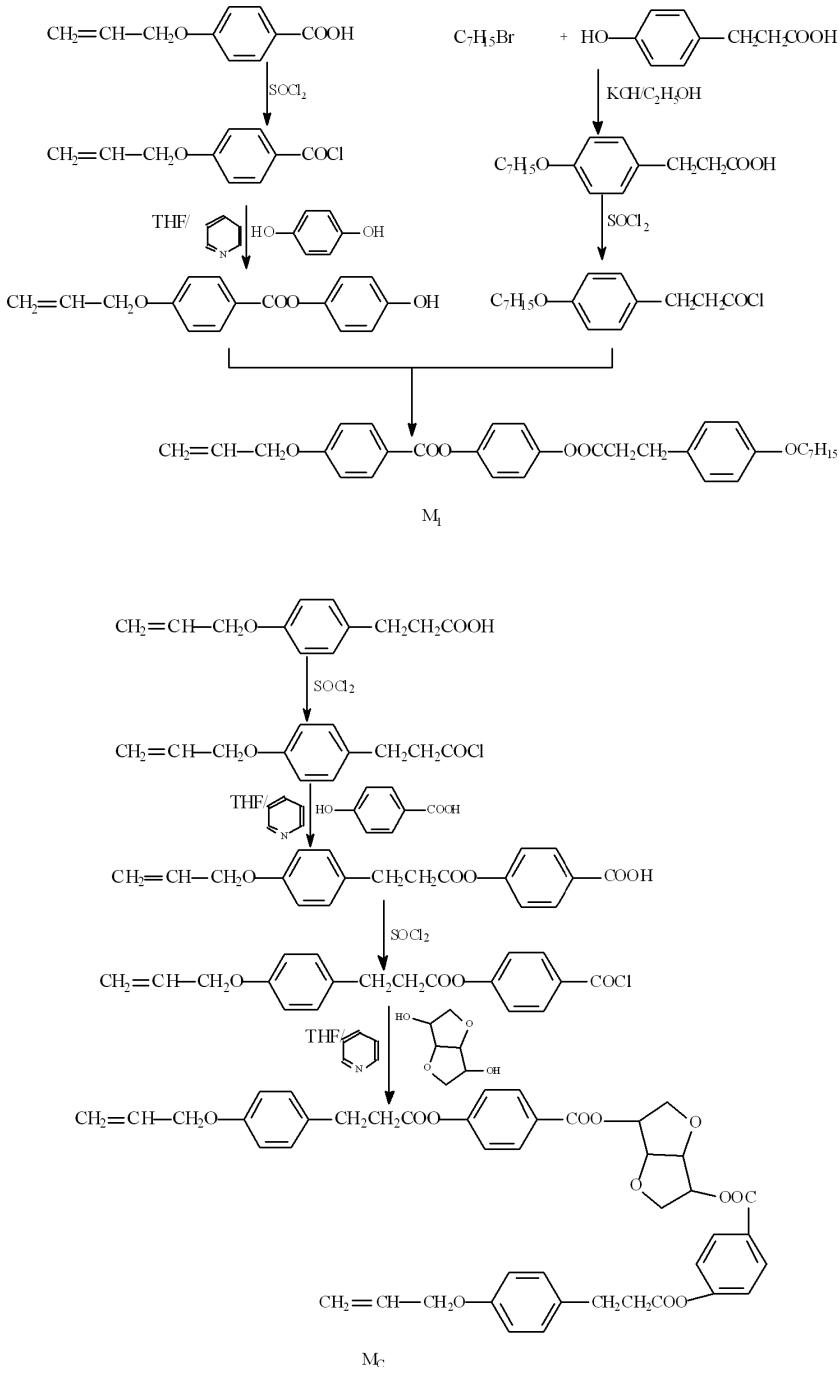

Scheme 1. Synthetic route of monomers.

IR(KBr): 3038 (=C-H), 2980, 285 0(-CH_3,-CH_2), 1746, 1723, (C=O) 1648 (C=C), 1605–1450 cm^{-1} (Ar-).

1H NMR ($CDCl_3$): δ 2.85–3.03 (m, 4H, -CH_2-CH_2-), 4.04–5.06 (m, 10H, isosorbide-H), 4.53–4.68 (d, 2H, CH_2=$CHCH_2O$), 5.31–5.46 (m, 2H, CH_2=CH-), 6.01–6.11 (m, 1H, CH2=CH-), 6.87–8.23 (m, 16H, Ar–H).

2.3.3 *Synthesis of the elastomers*

The synthetic routes of elastomers are outlined in Scheme 2. The mesogenic monomer and chiral cross-linking agent reacted with Si-H of PMHS to form elastomers in the presence of a Pt catalyst. All polymers synthesised are listed in Table 1. The monomer **M_I**, **M_C**, PMHS was dissolved in anhydrous, freshly distilled toluene. The mixture was heated to 65°C

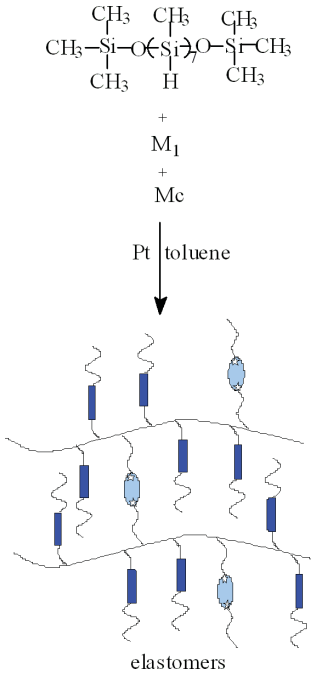

Scheme 2. Synthesis and schematic representation of elastomers $\mathbf{P_2}$–$\mathbf{P_7}$.

Table 1. Polymerization of $\mathbf{P_1}$–$\mathbf{P_8}$.

Polymer	Feed (mmol) $\mathbf{M_1}$	Feed (mmol) $\mathbf{M_C}$	$\mathbf{M_C}$[a] (mol%)	Yield (%)	Solubility[b] Toluene	xylene	DMF
$\mathbf{P_1}$	3.500	0.000	0	86.2	+	+	+
$\mathbf{P_2}$	3.360	0.070	2	83.5	–	–	–
$\mathbf{P_3}$	3.220	0.140	4	87.8	–	–	–
$\mathbf{P_4}$	3.080	0.210	6	88.6	–	–	–
$\mathbf{P_5}$	2.940	0.280	8	78.5	–	–	–
$\mathbf{P_6}$	2.800	0.350	10	79.1	–	–	–
$\mathbf{P_7}$	2.450	0.525	15	75.7	–	–	–
$\mathbf{P_8}$	2.100	0.700	20	68.8	–	–	–

[a]Molar fraction of $\mathbf{M_C}$ based on $\mathbf{M_1}$+$\mathbf{M_C}$.
[b]+ dissolve; – insolubility or swelling.

under nitrogen and anhydrous conditions, and then 2 ml of tetrahydrofuran solution of hexachloroplatinic acid (IV) catalyst (5 mg ml^{-1}) was injected with a syringe. The hydrosilication reaction followed the track of Si-H stretch intensity up to disappearance, and would be completed within 30 h, as indicated by IR, followed by precipitation with methanol. The products were desiccated in a vacuum at room temperature.

IR(KBr): 2980, 2850 (-CH_3, -CH_2), 1757, 1733 (C=O), 1605–1450 (Ar-), 1200–1000 cm^{-1} (Si–O–Si).

3. Results and discussion

3.1 Synthesis

Two novel monomers have been synthesised: a nematic monomer ($\mathbf{M_1}$) and a chiral crosslinking agent ($\mathbf{M_c}$). The reaction pathways to the $\mathbf{M_1}$ and $\mathbf{M_c}$ are shown in Scheme 1.

$\mathbf{M_1}$ was prepared by (1) etherification of 3-(4-hydroxyphenyl)propanoic acid with *n*-bromoheptane to give *3-[4-heptyloxy-phenyl]-propionic acid;* (2) esterification of 3-(4-hydroxyphenyl)propanoic acid chloride with 4-ally- loxybenzoic acid 4-hydroxy phenylester to give $\mathbf{M_1}$.

Mc was prepared by (1) etherification of 3-(4-hydroxyphenyl)propanoic acid with 3-bromopropene to give 4-[4-allyloxy-phenyl]-propionic acid; (2) esterification of 4-[4-allyloxy-phenyl]-propionic acid chloride with 4-hydroxy-benzoic acid to obtain 4-[3-[4-allyloxy-phenyl] propionyloxy] benzoic acid and then reacted with isosorbide to give $\mathbf{M_c}$. The chemical structure of the two monomers was characterised by Fourier Transform Infrared Spectroscopy (FTIR) and ^{1}H NMR spectroscopy. The FTIR of $\mathbf{M_1}$ and $\mathbf{M_c}$, respectively, showed characteristic bands at 1746–1723 cm^{-1} originating from ester C=O stretching, 1649 cm^{-1} due to olefinic C=C stretching, and 1605~1450 cm^{-1} corresponding to aromatic C=C stretching. The ^{1}H NMR spectra of $\mathbf{M_1}$ and $\mathbf{M_c}$ showed multiplets at 6.85–8.15 ppm, 5.30–6.11 ppm, 4.0–5.06 ppm, 2.84–3.03 ppm, and 0.882–1.80 ppm, corresponding to aromatic, olefinic protons, and methylene, isosorbide, methylene and methyl protons. The new series of chiral elastomers $\mathbf{P_2}$–$\mathbf{P_8}$ was prepared with a one-step hydrosilation reaction between Si-H groups of PMHS and olefinic C=C of nematic monomer and difunctional chiral crosslinking agent in toluene, using hexachloroplatinic acid catalyst at 60°C. The yields and properties of $\mathbf{P_2}$–$\mathbf{P_8}$ are summarised in Table 1. The obtained elastomers were insoluble in toluene, xylene, DMF, chloroform etc., but could swell in these solvents. The FTIR spectra of $\mathbf{P_1}$–$\mathbf{P_8}$ showed the complete disappearance of Si–H stretching band at about 2166 cm^{-1}. Characteristic absorption bands appeared at 1740–1728, 1605–1450 and 1200–1000 cm^{-1}, attaching to the stretching of ester C=O, aromatic, and Si–O–Si, respectively. It can be concluded that the chemical structures of obtained monomers and polymers are consistent with our expectations.

3.2 Thermal properties

The phase transition temperature and corresponding enthalpy changes are summarised in Table 2; DSC curves of monomer $\mathbf{M_1}$ and elastomer $\mathbf{P_3}$, $\mathbf{P_5}$, $\mathbf{P_7}$ are

Table 2. Thermal properties of polymer.

Polymer	T_g /°C	T_i /°C	ΔH/J g^{-1}	ΔT [a]	LC phase
P$_1$	55.4	144.1	2.757	88.7	Nematic
P$_2$	52.4	139.8	3.408	87.4	Cholesteric
P$_3$	50.1	132.1	3.758	82.0	Cholesteric
P$_4$	48.8	126.0	2.168	77.2	Cholesteric
P$_5$	48.0	119.6	1.527	71.6	Cholesteric
P$_6$	47.3	113.7	1.336	66.4	Cholesteric
P$_7$	46.6	96.0	0.379	49.4	Cholesteric
P$_8$	50.1	–	–	–	–

[a]T_i, the peak temperature between onset and end.
[b]Mesophase temperature ranges ($T_i - T_g$).

shown in Figure 1 (a) and (b). A melting transition and a nematic to isotropic phase transition for **M$_1$** appeared at 69.0 and 142.4°C. For the elastomers **P$_2$**–**P$_7$**, glass transition temperatures and cholesteric to isotropic transition temperatures appeared on DSC curves. As seen from the data in Table 2, low content of crosslinking agent did not significantly affect the phase behaviour of the elastomers, and reversible phase transitions were observed due to sufficient molecular motion. In contrast, higher content of crosslinking agent had a strong influence on the phase behaviour: it could cause the LC phase to disappear due to the disturbance of the mesogenic order. The DSC curve of **P$_8$** showed only a glass transition. Above all, the phase transitions are reversible and do not change on repeated heating and cooling cycles.

In general, crosslinking has two effects on the phase behaviour. On the one hand, it will impose additional constraints on the segment motion of polymer chains, and might be expected to raise the glass transition temperature; on the other hand, it will play a plasticiser role and might reduce the glass transition temperature. The two opposite effects bring about the counter balance and offer the different variable trend. Taking the crosslinking effect and plasticisation effect into account, T_g is given by

$$T_g = T_{go} + K_x f_x - K_y P_x,$$

where T_g and T_{go} are the glass transition temperature of crosslinked and uncrosslinked polymers, K_x and K_y, are constant, and f_x and P_x are the crosslink effect and the plasticiser effect, respectively, as the content of the crosslinking agent is x.

Figure 2 shows the effect of the concentration of crosslinking units on the phase transition temperature of **P$_1$**–**P$_8$**. It can be seen that the T_g value of **P$_1$** is higher, which is chiefly due to its molecular rigidity. When the chiral crosslinker is induced into the polymer first, the crosslinker's plasticisation effect is very obvious. The T_g values of **P$_1$**–**P$_3$** reduced from 55.4 to 50.1°C. The non-LC crosslinking agent had significant effects as plasticisation at first, which is due to the hard parent polymer. The T_g values of **P$_3$**–**P$_7$** reduced slowly from 50.1 to 46.6°C, which was the result of the equivalent between the dilute influence of plasticisation and the crosslinking effect. Finally, the T_g value of **P$_8$** rose again when the crosslinking effect became gradually predominant with x reaching a certain critical value.

Similarly to T_g, crosslinking may influence the clearing point (T_i) in two ways. First, crosslinking units may act as a non-mesogenic diluents and lead to a downward shift in the clearing point as increasing proportions are added to a liquid crystalline polymer. For a crosslinked sample, chemical crosslinking could prevent the motion and orientation of mesogenic

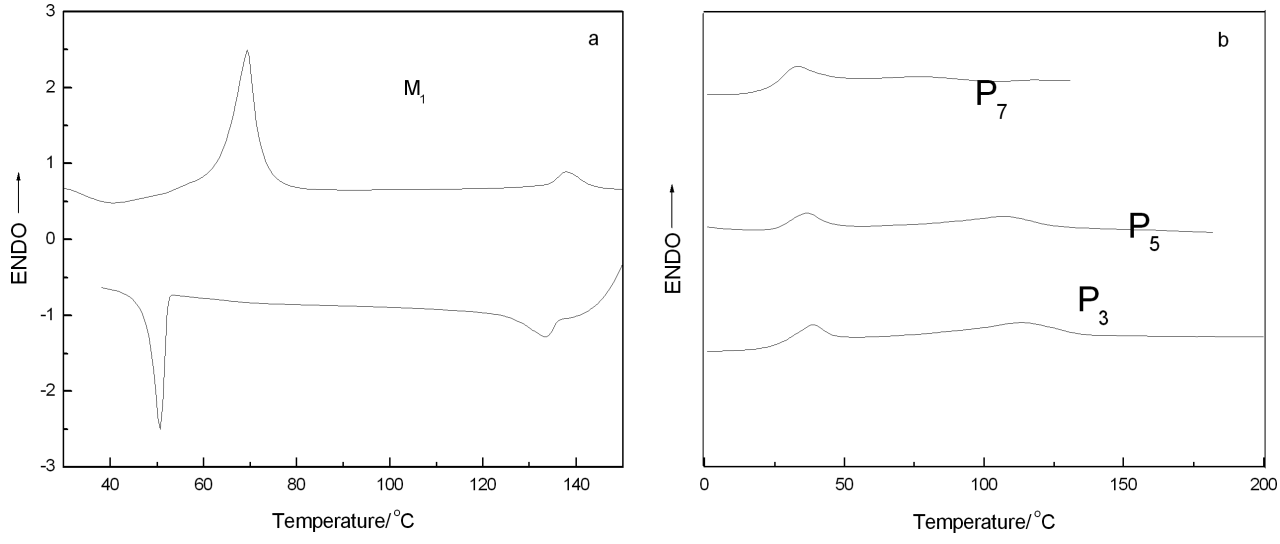

Figure 1. Thermographs of liquid crystal monomer (a) and elastomers (b).

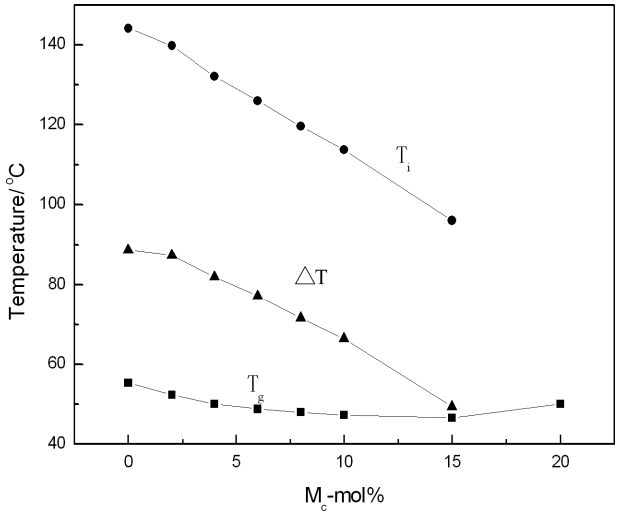

Figure 2. Effect of $\mathbf{M_c}$ content on phase transition temperature of the elastomers.

molecules and was not in favourable for the formation of mesogenic orientation order in the elastomers with increasing x. Secondly, for a crosslinked sample, heating to the isotropic state required additional energy to distort the polymer backbone from the anisotropic state at crosslinking and lead to a forward shift in the clearing point with increasing proportions of chiral crosslinking agent. In this study, the non-LC crosslinking agent is induced into the polymer backbone, so the first factor is predominant. It can be found that the clearing temperatures decreased from 144.1 to 96.0°C for $\mathbf{P_1}$–$\mathbf{P_8}$ when increasing x; mesophase temperature ranges (ΔT) of elastomers decreased also with increasing x. The temperatures at which 5% weight loss occurred (T_d) were greater than 300°C for $\mathbf{P_2}$–$\mathbf{P_8}$, which shows that the synthesised elastomers have high thermal stability.

3.3 *Optical properties*

It is well known that a cholesteric LC phase can be obtained when a nematic phase is doped with chiral molecules; the long axis of the liquid crystal molecules (the director n) rotates about a helix. Cholesteric LCEs, by inducing a chiral non-LC crosslinking agent and nematic LC monomers, were expected. In this phase a band of incident circularly polarised light has the same sense, as the cholesteric helix is reflected whereas the band with the opposite sense is transmitted. The wavelength of selective reflection of light λ obeys the Bragg condition:

$$\lambda = nP.$$

The reflected band width ($\Delta\lambda$) is given by:

$$\Delta\lambda = \lambda_{\max} - \lambda_{\min} = P \times (n_e - n_o),$$

where n_e and n_o are the extraordinary and the ordinary refractive indices of a uniaxially oriented phase respectively. In general, the helical pitch and optical properties of side-chain cholesteric liquid crystalline polymers depend on the polymer backbone, the rigidity of mesogen, the length of the flexible spacer, the copolymer composition, the molecular mass, and the outer conditions (such as temperature, force field, electric field and magnetic field). Although the microscopic origins of pitch are still a subject of study, it is well known that the pitch and the reflected colours depend on temperature. Two technologically relevant questions about cholesteric are how to adjust the pitch and how to keep it constant once it has the right value. The optical textures of the monomers and polymers are studied by POM with hot stage under nitrogen atmosphere. POM observation results showed that $\mathbf{M_1}$ exhibited enantiotropic nematic phase. When $\mathbf{M_1}$ was heated to 69°C, the sample began to melt, a typical nematic threaded texture gradually appeared and then disappeared at 142.2°C. When the isotropic state was cooled to 138.6°C, the small schlieren texture gradually occurred and disappeared quickly, and then a droplet texture appeared and step by step a threaded texture appeared again. The photomicrographs of $\mathbf{M_1}$ are shown in Figure 3 (a) and (b).

The uncrosslinked polymer $\mathbf{P_1}$ gradually showed a colourful texture and resulted in a needle-shaped texture when approaching the clearing point. The photomicrograph of $\mathbf{P_1}$ is shown in Figure 4(a). The needle-shaped texture did not appear for $\mathbf{P_2}$–$\mathbf{P_8}$ because of the existence of the motion-impeding crosslinker. For elastomers $\mathbf{P_2}$–$\mathbf{P_8}$, the molecular motion is not very free because of the long and rigid crosslinker, so the holding temperature process was necessary when the elastomers were characterised by POM and satisfactory results were obtained when they were held at liquid crystalline phase temperature for 1–2 h. They all became cholesteric Grandjean texture and all showed shrinkage when shearing. $\mathbf{P_3}$ exhibited Grandjean blue phase in the cooling cycle. $\mathbf{P_2}$–$\mathbf{P_3}$ showed transmitted colour, which is due to the proper pitch. $\mathbf{P_8}$ displayed stress-induced birefringence. The photomicrograph of $\mathbf{P_2}$ –$\mathbf{P_7}$ is shown in Figure 4 (b), (c) and (d). $\mathbf{P_2}$ –$\mathbf{P_7}$ are cholesteric phase as expected. Correct concentrations of chiral crosslinking agent with nematic LC can result in typical cholesteric LCEs.

3.4 *XRD analysis*

XRD analysis allowed for a complementary assessment of the nature of the phases observed by DSC

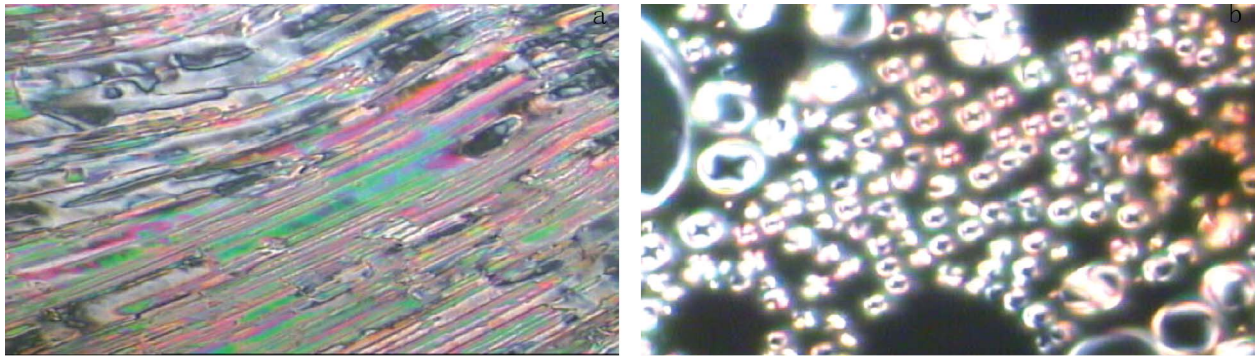

Figure 3. Optical texture of monomer $\mathbf{M_1}$. a) Threadlike texture of $\mathbf{M_1}$ at heating to 124.3°C; b) cross-like droplet texture of $\mathbf{M_1}$ at cooling to 126.4°C.

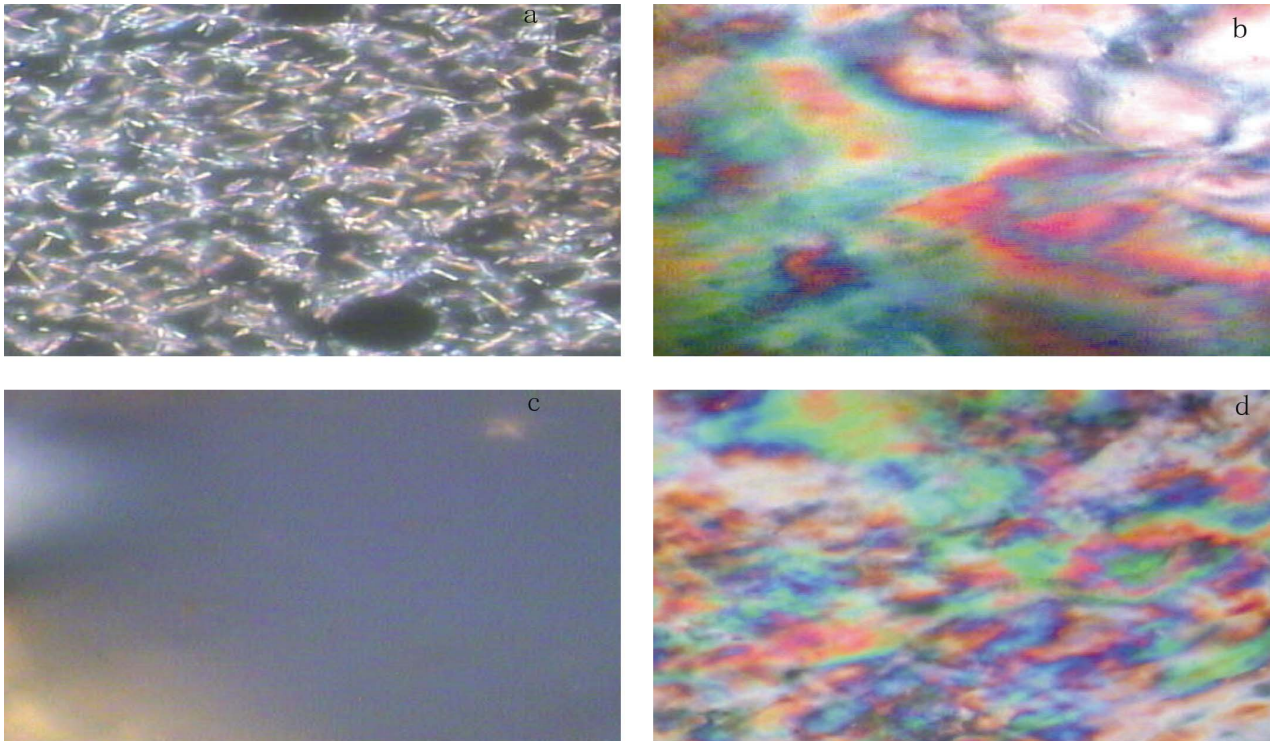

Figure 4. Optical texture of elastomers. a) Needle-like texture of $\mathbf{P_1}$ at heating to 156.5°C; b) Grandjean texture of $\mathbf{P_1}$ at heating to 154.5°C; c) Grandjean blue texture of $\mathbf{P_3}$ at cooling to 77.7°C; d) Grandjean texture of $\mathbf{P_4}$ at heating to 112.1°C.

and POM, giving additional information about their structural parameters. WAXD patterns of polymers are shown in Figure 5. These samples were quenched from the liquid crystal phase. In general, a smectic, nematic, cholesteric structure has a broad peak associated with lateral packing at $2\theta \approx 16$–20° in a wide-angle X-ray diffraction (WAXD) curve. A sharp strong peak at a low angle ($1^\circ < 2\theta < 4^\circ$) in small-angle X-ray scattering (SAXS) curve can be observed for the smectic structure, but it cannot be seen for nematic and cholesteric structures. For $\mathbf{P_1}$–$\mathbf{P_8}$, a sharp peak associated with the smectic layers at a low angle did not appear in the SAXS curve and a weak peak and a broad peak were observed, respectively, at 22.47–23.08° (d = 7.9–7.69 Å) in WAXD. As the level of crosslinking agent increased, these broad peaks became weaker; this is simply related to the difference between the intrachain scattering of the mesogenic repeat and the crosslinking unit. The nematic phase structure of $\mathbf{P_1}$, and the cholesteric phase structures of $\mathbf{P_2}$–$\mathbf{P_7}$ were confirmed by optical texture and XRD results.

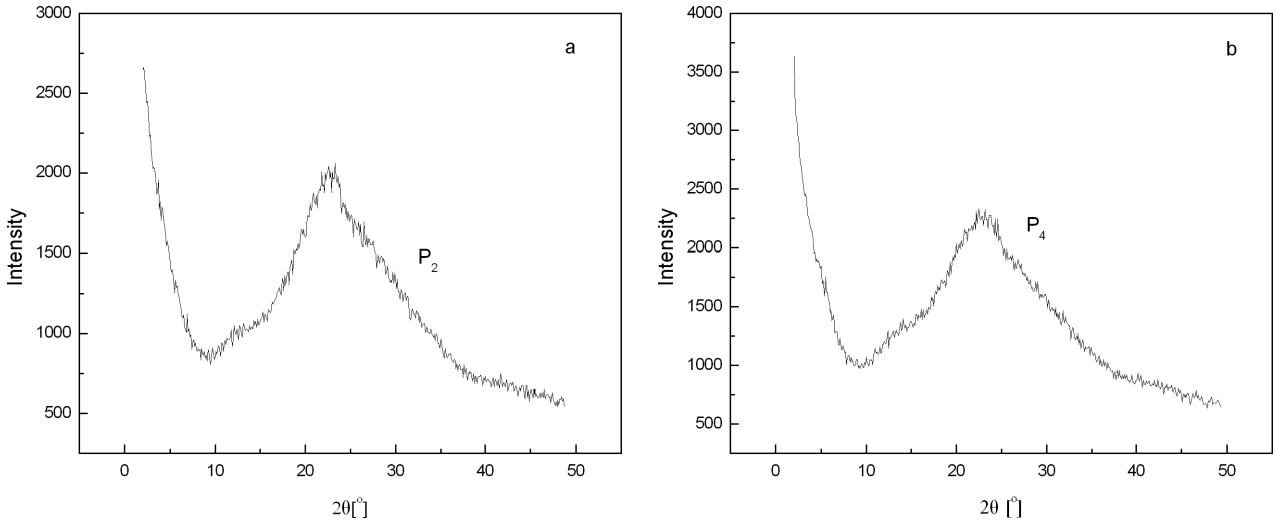

Figure 5. X-Ray diffraction patterns of quenched samples of elastomers.

4. Conclusions

In this study, a series of new side-chain cholesteric LCEs containing nematic liquid crystal monomer $\mathbf{M_1}$, 4-allyloxy-benzoic acid-4-[3-[4-heptyloxy-phenyl] -propionyloxy-phenylester, and $\mathbf{M_C}$, hexahydro-furo[3,2-b]furan-3,6-diyl- bis[4-[3-[4-allyloxy]phenyl]-propanoyloxy]benzoate, were synthesised and characterised. The structures of monomers and elastomers are consistent with our designed. It can be concluded that lightly chemical crosslinker can few affect phase behaviour of the elastomers and cholesteric elastomers with Grandjean texture were yielded by introduction chiral crosslinking agent into polymer. The elastomers showed elasticity, reversible phase transition and Grandjean texture during heating and cooling cycles and can be obtained by shearing when holding at LC phase for 2 h. Selective reflection of light can be seen for $\mathbf{P_2}$–$\mathbf{P_3}$. $\mathbf{P_3}$ showed Grandjean blue texture when cooling. For $\mathbf{P_1}$–$\mathbf{P_8}$, the glass transition temperature first reduced and then increased, the isotropisation temperature and the ranges of the mesophase temperature decreased with increasing content of crosslinking reagent.

Acknowledgments

The authors are grateful to the National Natural Science Fundamental Committee of China and HI-Tech Research and Development Program (863) of China, to the China Postdoctoral Science Foundation, and Postdoctoral Science and Research Foundation of Northeastern University for financial support of this work, and to Shen Yang Scientific and Technical Bureau Foundation.

References

(1) Finkelmann, H.; Kock, H.J.; Rehage, G. *Makromol. Chem. Rapid Commun.* **1981**, *2*, 317–322.
(2) Zentel, R.; Reckert, G. *Makromol. Chem.* **1986**, *187*, 1915–1926.
(3) Mitchell, R.; Davis. J. *Polymer* **1987**, *28*, 639–647.
(4) Zentel, R. *Angew. Chem. Adv. Mater.* **1989**, *101*, 1437–1445.
(5) Loffler, R.; Finkelman, H. *Macromol. Chem. Rapid Commun*. **1990**, *11*, 321–326.
(6) Broer, D.J.; Heynderickx. I. *Macromolecules* **1990**, *23*, 2474–2477.
(7) Davis, J. *J. Mater. Chem.* **1993**, *3*, 551–562.
(8) Broer, D.J.; Lub, J.; Mol, G.N. *Nature* **1995**, *378*, 467–469.
(9) Peter, P.M. *Nature* **1998**, *391*, 745–749.
(10) Hikmet, R.A.M.; Kemperman, H. *Nature* **1998**, *392*, 476–479.
(11) Maxein, G.; Mayer, S.; Zentel, R. *Macromolecules* **1999**, *32*, 5747–5754.
(12) Thomas, P.; Kurschner, K.; Strohriegl, P. *Macromol. Chem. Phys*. **1999**, *200*, 2480–2486.
(13) Kihara, H.; Kato, T.; Uryu, T.; Frechet, J.M.J: *Liq. Cryst.* **1998**, *24*, 413–418.
(14) Dirk, H.; Holger, F.; Rolf, M.; Klee, J.E. *Adv. Mater.* **1998**, *11*, 864–873.
(15) Stockley, J.E.; Sharp, G.D.; Serati, S.A.; Johnson, K.M. *Opt. Lett.* **1995**, *20*, 2441–2443.
(16) Sapich, B.; Stumpe, J.; Krawinkel, T.; Kricheldorf, H.R. *Macromolecules* **1998**, *31*, 1016–1023.
(17) Finkelmann, H. *Adv. Mater*. **2001**, *13*, 1069–1072.
(18) Zhang, B.Y.; Hu, J.S.; Jia, Y.G.; Du, B.G. *Macromol. Chem. Phys.* **2003**, *204*, 2123–2129.
(19) Hu, J.S.; Zhang, B.Y.; Sun, K.; Li, Q.Y.; *Liq. Cryst.* **2003**, *30*, 1267–1274.
(20) Meng, F.B.; Zhang, B.Y.; Liu, L.M.; Zang, B.L. *Polymer* **2003**, *44*, 3935–3943.
(21) He, X.Z.; Zhang, B.Y.; Meng, F.B,; Lin., J.R. *J. Appl. Polym. Sci.* **2005**, *96*, 1204–1210.
(22) Kricheldorf, H.R.; Krawinkel, T. *Macromol. Chem. Phys.* **1998**, *199*, 783–790.